Supporting Information

Reticular synthesis of bcu topological hydrogen-bonded organic frameworks for white-light-emission

Xiao-Juan Xi,[a] Yang Li,[b] Feifan Lang,[b] Jiandong Pang*[b] and Xian-He Bu*[a,b]

[a] *College of Chemistry, State Key Laboratory of Elemento-Organic Chemistry, Nankai University, Tianjin 300071, P. R. China.*

[b] *School of Materials Science and Engineering, Smart Sensing Interdisciplinary Science Center, TKL of Metal and Molecule-Based Material Chemistry, Collaborative Innovation Center of Chemical Science and Engineering, Nankai University, Tianjin 300350, P. R. China.*

∗ Corresponding authors

E-mail address: jdpang@nankai.edu.cn (J. Pang), buxh@nankai.edu.cn (X.-H. Bu)

All chemicals and reagents were received from commercial suppliers and were used directly without additional purification. ^{1}H NMR spectra were recorded on a Bruker AV400 Nuclear Magnetic Resonance Spectrometer. Single-crystal X-ray diffraction analysis (SCXRD) were performed on a Rigaku XtalAB PRO MM007 DW diffractometer (Cu-Ka λ = 1.54178 Å). Powder X-ray diffraction (PXRD) test were carried out using a Rigaku MiniFlex600 diffractometer equipped with a Cu-target tube at 40 kV and 15mA. PXRD tests at 100 K were conducted on a a Rigaku XtalAB PRO MM007 DW diffractometer (Cu-Ka λ = 1.54178 Å). Specifically, the crystals were picked out from the mother liquid, transferred to the oil, crushed with a needle, and then mounted on the loop ring for PXRD determination at 100 K. The thermogravimetric analyses (TGA) were conducted on a Rigaku Thermo Plus EVO2 8121 thermal analyzer. UV-vis absorption spectra were obtained using a Thermo scientific UV-vis Evolution 220 spectrophotometer. Fourier transform infrared (FTIR) spectra were recorded on a TENSOR 37 spectrometer. The photoluminescence (PL) spectra, PL decay curve, and absolute photoluminescence quantum yields were measured on an Edinburgh instruments FS5 spectrophotometer. The ESP diagram based on single-crystal structure was obtained by the Material Studio software using the gradient approximation (GGA) with the Perdew-Burke-Ernzerhof (PBE) functional in Dmol3 module. The size of the dye molecules was calculated by bringing the atomic coordinates of the dye molecule obtained in the Chem3D software into the small program on the web page http://jerkwin.github.io/2016/06/24/%E5%88%86%E5%AD%90%E5%B0%BA%E5%AF%B8%E5%A4%A7%E5%B0%8F%E7%9A%84%E8%AE%A1%E7%AE%97/

Experimental Procedures

Synthesis of H_8PEP-OBu

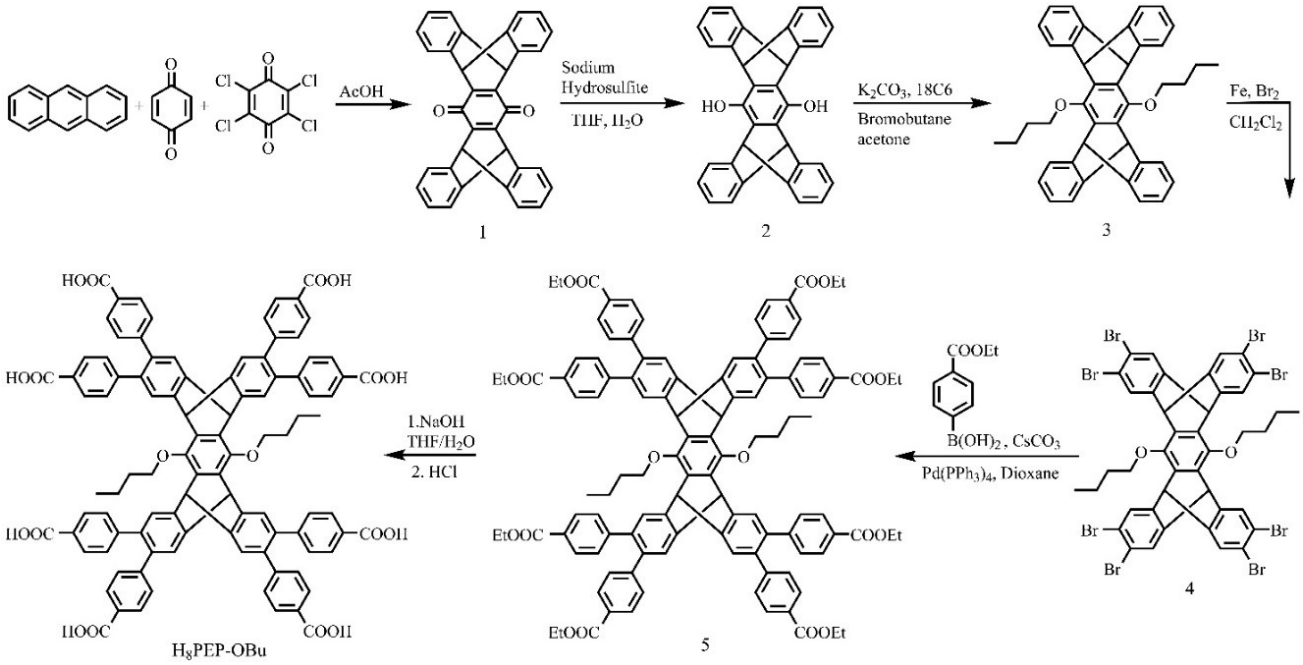

Scheme S1 Synthesis of H_8PEP-OBu.

Synthesis of compound 1. Anthracene (10.69 g, 60 mmol), 1,4-benzoquinone (3.24 g, 30 mmol), and p-chloranil (14.75 g, 60 mmol) were dissolved in acetic acid (300 mL). The mixture was stirred at 125 °C for 16 h. After cooled to room temperature, the mixture was poured into water (300 mL). The residue was collected by filtration, washed several times by hot water, and dried under vacuum to afford yellow powder (13.11 g, yield: 95%). ^{1}H NMR (400 MHz, $CDCl_3$): δ 7.37 (d, 8H), 6.98 (d, 8H), 5.75 (s, 4H) ppm.

Synthesis of compound 2. Compound 1 (7.82 g, 17 mmol) was dissolved in 200 mL anhydrous tetrahydrofuran, followed with the addition of 140 mL sodium hydrosulfite (35.52 g, 204 mmol) aqueous solution. The reaction mixture was heated at 40 °C for 15 h under N_2 atmosphere and then cooled to room temperature. Tetrahydrofuran was removed using rotary evaporation and resulting precipitate was filtered and washed sequentially with hot water and acetone, and dried under 50 °C to afford white powder (7.67 g, 98%). ^{1}H NMR (400 MHz, $CDCl_3$): δ 7.33 (d, 8H), 6.94 (d, 8H), 5.64 (s, 4H) ppm.

Synthesis of compound 3. Compound 2 (7.67 g, 16.60 mmol), K_2CO_3 (11.47 g, 83 mmol), and catalytic amount of 18-crown-6 (18C6) (50 mg), bromobutane (16.10 ml, 150 mmol) were dissolved in acetone (300 mL). The reaction mixture was heated at 65 °C for 15 h under N_2 atmosphere and then cooled to room temperature. Acetone was removed using rotary evaporation and resulting precipitate was washed with hot water, and dried under vacuum to afford white powder (7.67 g, 95%). ^{1}H NMR (400 MHz, $CDCl_3$): δ 7.32 (d, 8H), 6.94 (d, 8H), 5.64 (s, 4H), 3.90 (t, 4H), 1.99 (m, 4H), 1.73 (m, 4H), 1.14 (t, 6H) ppm.

Synthesis of compound 4. Compound 3 (57.4 mg, 1 mmol) and catalytic amount iron filings (160 mg) were dissolved in 60 mL anhydrous CH_2Cl_2 (60 mL) in a dried 100 mL flask. Then, bromine (0.53 mL, 9.7 mmol) was added to the flask. The reaction mixture was heated at 45 °C for 1.5 h under N_2 atmosphere and then cooled to room temperature. The mixture was washed with sodium thiosulfate aqueous solution and then extracted with CH_2Cl_2. The organic phase was purified by chromatography to give yellow solid, which was washed with ethanol to provide 4 as pale yellow solid (890 mg, 74%). ^{1}H NMR (400 MHz, $CDCl_3$): δ 7.56 (s, 8H), 5.51 (s, 4H), 3.86 (t, 4H), 1.96 (m, 4H), 1.72 (m, 4H), 1.50 (m, 4H), 1.16 (t, 6H) ppm.

Synthesis of compound 5. Compound 4 (2.55 g, 2 mmol), (4-(ethoxycarbonyl)phenyl)boronic acid (4.66 g, 24 mmol), $CsCO_3$ (10.43 g, 32 mmol), and tetrakis(triphenylphosphine)palladium (0.46 g, 0.4 mmol) were added to a 500-mL Schlenk flask. The flask was pumped under vacuum and refilled with N_2 three times before 250 mL degassed 1,4-dioxane was transferred to the system. The reaction mixture was heated to 85 °C for 72 h under a N_2 atmosphere. After the reaction mixture cooled to room temperature, the organic solvent was removed using a rotary evaporator, and the resulting mixture was poured into water and extracted with CH_2Cl_2 (3×50 mL). The combined organic layers were dried over anhydrous $MgSO_4$, and then the solvent was removed using a rotary evaporator. After purification by column chromatography on silica gel using CH_2Cl_2 as eluent and evaporation of fraction containing the product, compound 5 was

obtained as a pale yellow solid (1.66 g, 45%). ^{1}H NMR (400 MHz, $CDCl_3$): δ 7.85 (d, 16H), 7.48 (s, 8H), 7.08 (d, 16H), 5.89 (s, 4H), 4.35 (q, 16H), 3.75 (t, 4H), 2.02 (m, 4H), 1.72 (m, 4H), 1.36 (t, 24H), 1.25 (t, 6H) ppm.

Synthesis of compound H_8PEP-OBu. Compound 5 (1.66 g, 0.9 mmol) was dissolved in 40 mL of THF, to which 40 mL of NaOH (2.16 g, 54 mmol) aqueous solution was added. The mixture was heated to 70 °C for 10 h, and then the organic solvent was removed using a rotary evaporator. The aqueous phase was acidified to pH = 3 using HCl. The resulting precipitate was collected via filtration, washed with water several times, and dried under vacuum to afford H_8PEP-OBu (1.33 g, 96%). ^{1}H NMR (400 MHz, DMSO-d_6): δ 12.92 (s, 8H), 7.75 (d, 16H), 7.57 (s, 8H), 7.15 (d, 16H), 6.06 (s, 4H), 4.03 (t, 4H), 1.97 (m, 4H), 1.68 (m, 4H), 1.01 (t, 6H) ppm.

Synthesis of H_8PEP-OMe

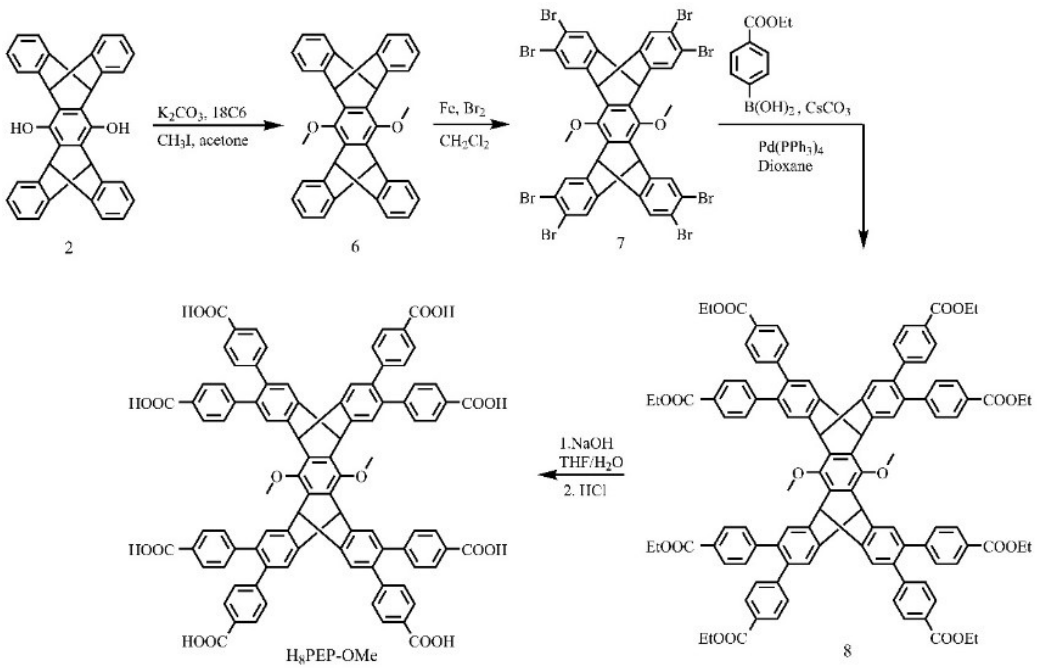

Scheme S2 Synthesis of H_8PEP-OMe.

Synthesis of compound 6. Compound 2 (0.93 g, 2 mmol), K_2CO_3 (1.38 g, 10 mmol), and catalytic amount of 18-crown-6 (6 mg), and methyl iodide (1.1 mL, 18 mmol) were dissolved in acetone (35 mL). The reaction mixture was heated at 65 °C for 15 h under N_2 atmosphere and then cooled to room temperature. Acetone was removed using rotary evaporation and resulting precipitate was washed with hot water, and cried under vacuum to afford white powder (0.75 g, 76%). ^{1}H NMR (400 MHz, $CDCl_3$): δ 7.35 (d, 8H), 6.96 (d, 8H), 5.68 (s, 4H), 3.88 (s, 6H) ppm.

Synthesis of compound 7. Compound 6 (490 mg, 1 mmol) and catalytic amount iron filings (160 mg) were dissolved in 60 mL anhydrous CH_2Cl_2 (60 mL) in a dried 100 mL flask. Then, bromine (0.53 mL, 9.7 mmol) was added to the flask. The reaction mixture was heated at 45 °C for 1.5 h under N_2 atmosphere and then cooled to room temperature. The mixture was washed with sodium thiosulfate aqueous solution and then extracted with CH_2Cl_2. The organic phase was purified by chromatography to give yellow solid, which was washed with ethanol to provide 7 as pale yellow solid (835 mg, 75%). ^{1}H NMR (400 MHz, $CDCl_3$): δ 7.58 (s, 8H), 5.54 (s, 4H), 3.86 (s, 6H) ppm.

Synthesis of compound 8. Compound 7 (2.24 g, 2 mmol), (4-(ethoxycarbonyl)phenyl)boronic acid (4.66 g, 24 mmol), $CsCO_3$ (10.43 g, 32 mmol), and tetrakis(triphenylphosphine)palladium (0.46 g, 0.4 mmol) were added to a 500-mL Schlenk flask. The flask was pumped under vacuum and refilled with N_2 three times before 250 mL degassed 1,4-dioxane was transferred to the system. The reaction mixture was heated to 85 °C for 72 h under a N_2 atmosphere. After the reaction mixture cooled to room temperature, the organic solvent was removed using a rotary evaporator, and the resulting mixture was poured into water and extracted with CH_2Cl_2 (3×50 mL). The combined organic layers were dried over anhydrous $MgSO_4$, and then the solvent was removed using a rotary evaporator. After purification by column chromatography on silica gel using CH_2Cl_2 as eluent and evaporation of fraction containing the product, compound 8 was obtained as a pale yellow solid (2.48 g, 74%). ^{1}H NMR (400 MHz, $CDCl_3$): δ 7.85 (d, 16H), 7.51 (s, 8H), 7.09 (d, 16H), 5.91 (s, 4H), 4.34 (q, 16H), 3.98 (s, 6H), 1.39 (t, 24H) ppm.

Synthesis of compound H_8PEP-OMe. Compound 8 (2.48 g, 1.5 mmol) was dissolved in 40 mL of THF, to which 40 mL of NaOH (3.6 g, 90 mmol) aqueous solution was added. The mixture was heated to 70 °C for 10 h, and then the organic solvent was removed using a rotary evaporator. The aqueous phase was acidified to pH = 3 using HCl. The resulting precipitate was collected via filtration, washed with water several times, and dried under vacuum to afford H_8PEP-OMe (2.07 g, 95%). ^{1}H NMR (400 MHz, DMSO-d_6): δ 7.75 (d, 16H), 7.61 (s, 8H), 7.15 (d, 16H), 6.11 (s, 4H), 3.94 (s, 6H) ppm.

Synthesis of HOFs

Synthesis of NKM-HOF-1: H_8PEP-OBu (15 mg), THF (6 mL), and methyl benzoate (MB) (3 mL) were charged in a 20 ml Pyrex vial. The mixture was heated in an 80 °C oven for 3 days, crystals of NKM-HOF-1 were harvested (yield: 68%).

Synthesis of NKM-HOF-2: H_8PEP-OMe (15 mg), THF (6 mL), and methyl benzoate (MB) (3 mL) were charged in a 20 ml Pyrex vial. The mixture was heated in an 80 °C oven for 3 days, crystals of NKM-HOF-1 were harvested (yield: 65%).

Single-crystal X-ray diffraction analysis (SCXRD)

All as-crystals were picked out from the mother liquid, transferred to oil, and mounted on the loop ring for SCXRD. For NKM-HOF-1 and NKM-HOF-2, diffraction data were tested on a Rigaku XtalAB Pro MM007 DW diffractometer equipped with Cu-Kα radiation (λ = 1.54184 Å) at 100 K. Data collection and reduction were conducted using the program CrysAlisPro.[1] The structures were solved using intrinsic phasing methods (SHELXT-2018/3), and refined by full-matrix least-squares on F^2 using OLEX2. [2, 3] Imposed restraints of each structure were described in the CIF files. Therefore, only the basic strategy of structural refinement is presented here. All non-hydrogen atoms were refined anisotropically, and the hydrogen atoms were included on geometrically calculated positions. Crystal data are summarized in Table S1 and S2. Crystal data have been deposited at the Cambridge Crystallographic Data Centre (CCDC), under CCDC numbers of 2311161 and 2311164.

Results and Discussion

Table S1 Crystallographic data and structure refinement for NKM-HOF-1 and NKM-HOF-2.

Identification code	NKM-HOF-1	NKM-HOF-2
CCDC number	2311161	2311164
Empirical formula	$C_{122}H_{94}O_{24}$	$C_{116}H_{82}O_{24}$
Formula weight	1943.97	1859.81
Temperature/K	99.99(10)	99.98(10)
Crystal system	orthorhombic	orthorhombic
Space group	Pnma	Pnma
a/Å	18.3338(5)	18.3974(3)
b/Å	25.9671(7)	26.3784(3)
c/Å	37.9645(8)	37.7312(4)
α/°	90	90
β/°	90	90
γ/°	90	90
Volume/Å^3	18074.0(8)	18310.7(4)
Z	4	4
ρ_{calcg}/cm^3	0.714	0.675
μ/mm^{-1}	0.406	0.388
F(000)	4072.0	3880.0
Crystal size/mm^3	0.3 × 0.2 × 0.1	0.3 × 0.2 × 0.1
Radiation	Cu K*α* (λ = 1.54184)	Cu K*α* (λ = 1.54184)
2Θ range for data collection/°	4.656 to 151.672	4.088 to 152.544
Index ranges	$-23 \le h \le 21$, $-32 \le k \le 15$, $-43 \le l \le 47$	$-22 \le h \le 23$, $-32 \le k \le 15$, $-47 \le l \le 45$
Reflections collected	67768	71805
Independent reflections	18526 [R_{int} = 0.0370, R_{sigma} = 0.0306]	18813 [R_{int} = 0.0264, R_{sigma} = 0.0259]
Data/restraints/parameters	18526/181/729	18813/39/677
Goodness-of-fit on F2	1.382	1.361
Final R indexes [I>=2σ (I)]	R_1 = 0.1155, wR_2 = 0.3421	R_1 = 0.1085, wR_2 = 0.3230
Final R indexes [all data]	R_1 = 0.1348, wR_2 = 0.3628	R_1 = 0.1221, wR_2 = 0.3410
Largest diff. peak/hole / e Å^{-3}	0.61/-0.65	0.55/-0.59

$R_1 = \sum||F_0|-|F_c||/\sum|F_0|$. $wR_2 = [\sum w(F_0^2-F_c^2)^2/\sum w(F_0^2)^2]^{1/2}$

Table S2 O···H hydrogen bond lengths and O-H···O bond angles in NKM-HOF-1 and NKM-HOF-2.

NKM-HOF-1					
O···H	Distance (Å)	O···O	Distance (Å)	O-H···O	Angle (°)
O14-H7#2	1.807	O5-O11#2	2.573	O5-H5-O11#2	173.3
O11#2-H5	1.737	O7#2-O14	2.632	O7#2-H7-O14	166.8
O9#3-H2	1.802	O2-O9#3	2.637	O2-H2-O9#3	172.2
O8-H12#3	1.772	O12#3-O8	2.605	O12#2-H12#3-O8	170.8
O9-H2#1	1.802	O2#1-O9	2.637	O12-H12-O8#1	170.8
O8#1-H12	1.772	O12-O8#1	2.605	O2#1-H2#1-O9	172.1
O11-H5#4	1.737	O5#4-O11	2.573	O7-H7-O14#4	166.8
O14#4-H7	1.807	O7-O14#4	2.632	O5#4-H5#4-O11	173.3
NKM-HOF-2					
O···H	Distance (Å)	O···O	Distance (Å)	O-H···O	Angle (°)
O2#3-H11	1.806	O7-O12#2	2.634	O7-H7-O12#2	176.7
O2-H11#1	1.806	O7#4-O12	2.634	O5#2-H5#2-O3	158.3
O12#2-H7	1.795	O11#1-O2	2.630	O8#3-H8#3-O14	163.8
O12-H7#4	1.795	O11-O2#3	2.630	O11-H11-O2#3	166.8
O3-H5#2	1.779	O5-O3#4	2.578	O5-H5-O3#4	158.3
O3#4-H5	1.779	O5#2-O3	2.578	O7#4-H7#4-O12	176.7
O14#1-H8	1.760	O8#3-O14	2.578	O11#1-H11#1-O2	166.8
O14-H8#3	1.760	O8-O14#1	2.578	O8-H8-O14#1	163.8

Symmetry codes: #1: *3/2-x, 1-y, 1/2+z*; #2: *1/2-x, 1-y, -1/2+z*; #3: *3/2-x, 1-y, -1/2+z*; #4: *1/2-x, 1-y, 1/2+z*

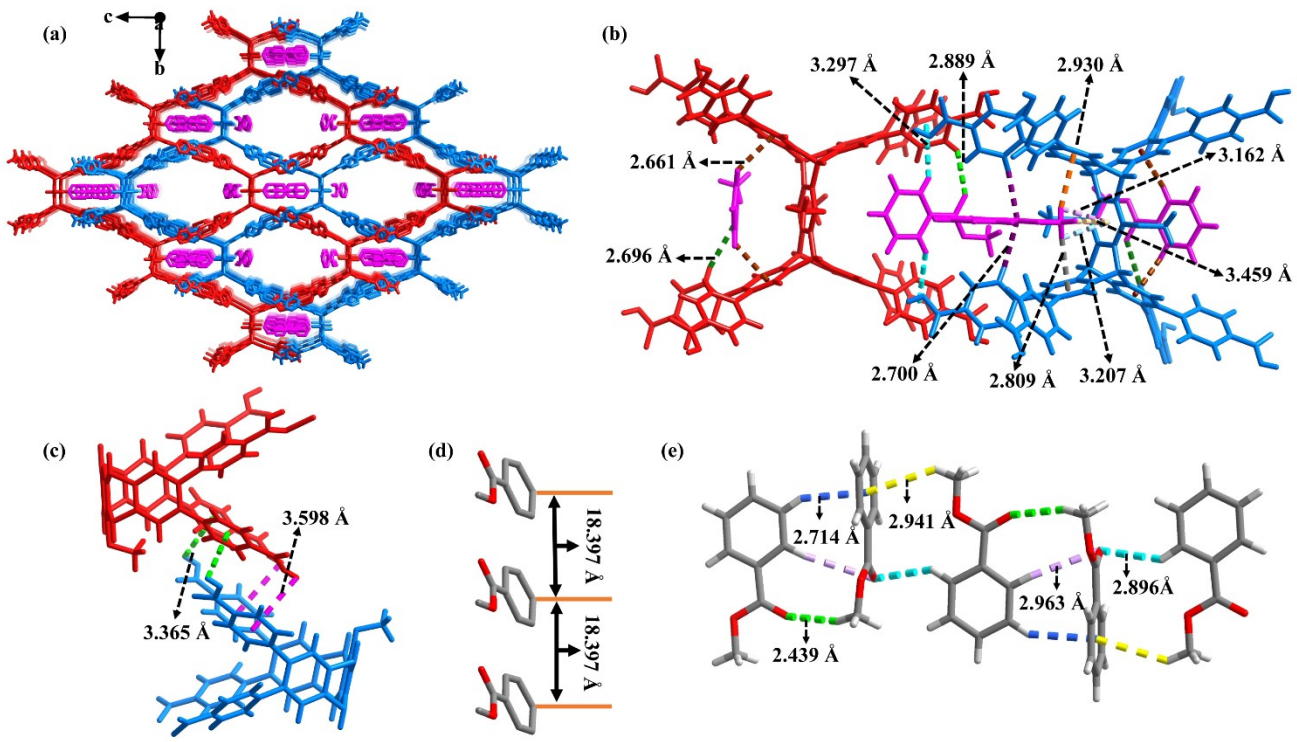

Fig. S1 (a) SCXRD structure of NKM-HOF-2 showing its 2-fold interpenetrated 3D supramolecular framework. Two sets of independent networks are plotted in red and light blue. The pores are filled with two types of MB molecules, which are plotted in pink. H atoms are omitted for clarity. (b) Illustration of the multiple C-H···π interactions formed among MB molecules and adjacent H_8PEP-OMe molecules (Green dotted lines: stronger interactions; Cyan dotted lines: weaker interactions). (c) Illustration of the multiple C-H···π interactions between adjacent H_8PEP-OMe molecules. (d) The parallel arranged MB molecules in the large pores of NKM-HOF-2. (e) The MB molecules packed in the form of -[A-B-C-D]- in the small pores of NKM-HOF-2.

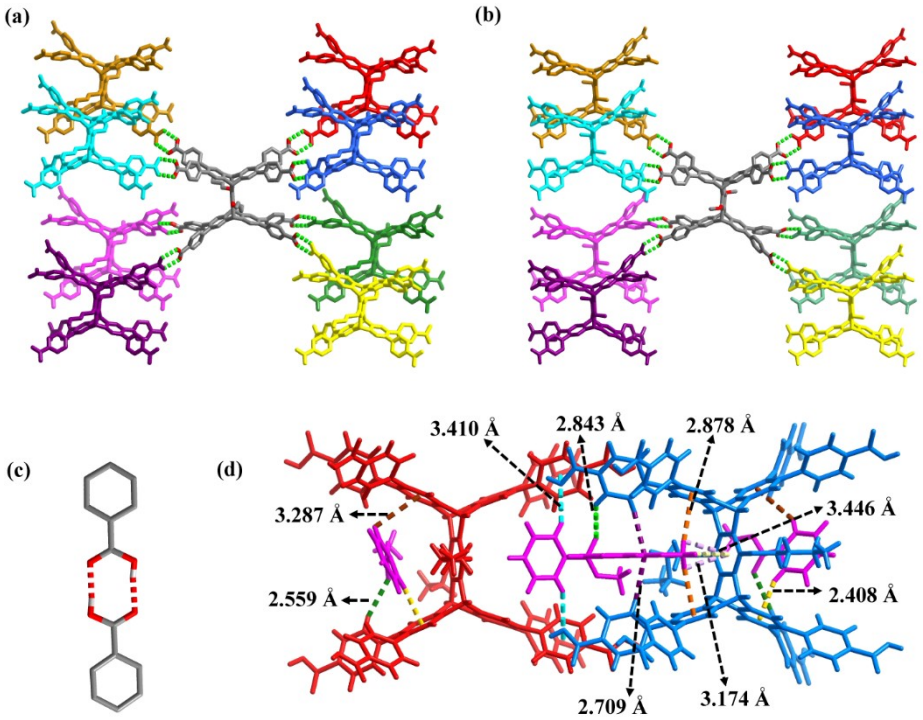

Fig. S2 (a) Each H_8PEP-OBu molecule in NKM-HOF-1 is connected to eight adjacent H_8PEP-OBu molecules via C-H···O hydrogen bonds. (b) Each H_8PEP-OMe molecule in NKM-HOF-2 is connected to eight adjacent H_8PEP-OMe molecules via C-H···O hydrogen bonds. (c) The hydrogen-bonding pattern of the carboxyl group in NKM-HOF-1 and NKM-HOF-2. (d) The MB molecules form multiple C-H···π interactions with adjacent H_8PEP-OBu molecules in NKM-HOF-1.

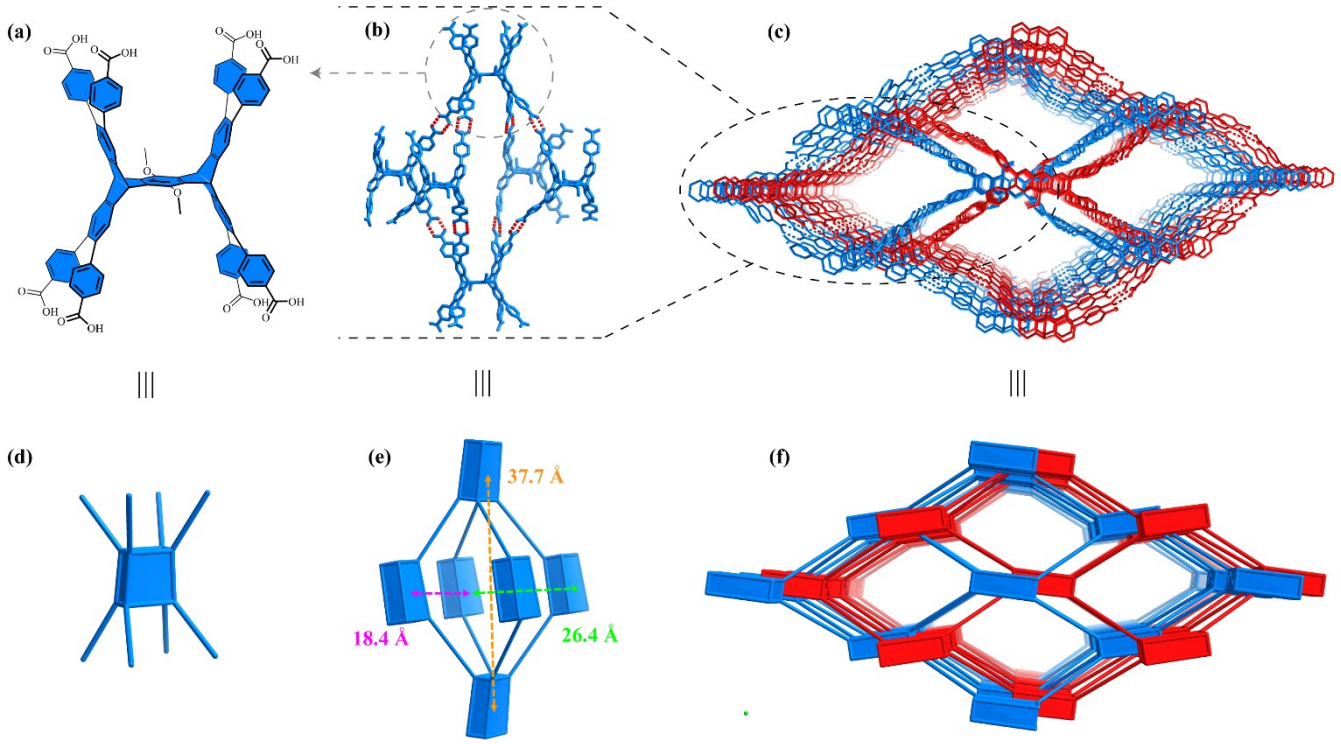

Fig. S3 (a) The structure of H_8PEP-OMe. (b) The octahedral cavities viewed from crystal structure (red dotted lines represent H-Bonds). (c) 2-fold interpenetrated frameworks of NKM-HOF-2 (each color represents an individual bcu net). (d) The 8-c quadrangular prism nodes simplified from H_8PEP-OMe. (d) The octahedral cavities viewed from topological structure. (f) A simplified single-node 8-c bcu topology.

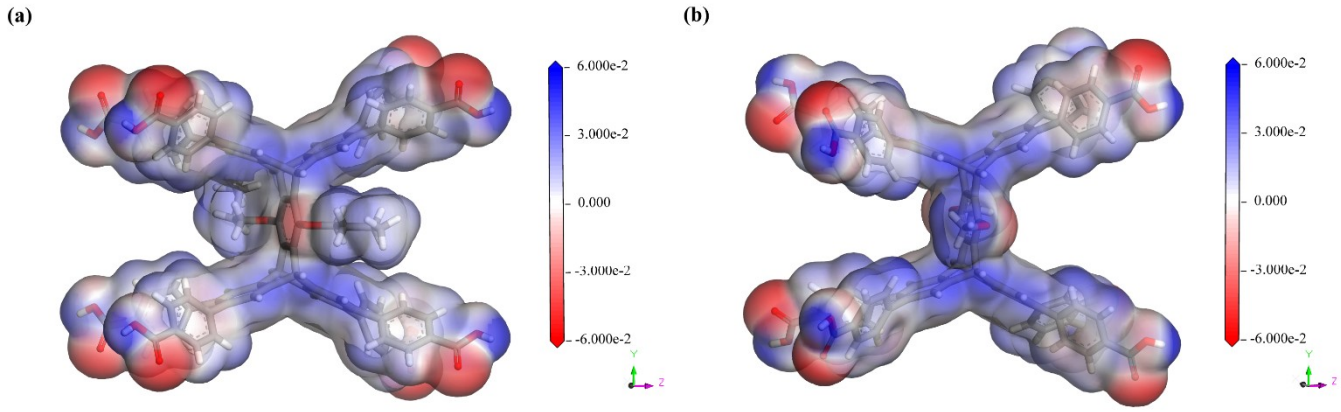

Fig. S4 Electrostatic potential (ESP) diagram of (a) NKM-HOF-1 and (b) NKM-HOF-2.

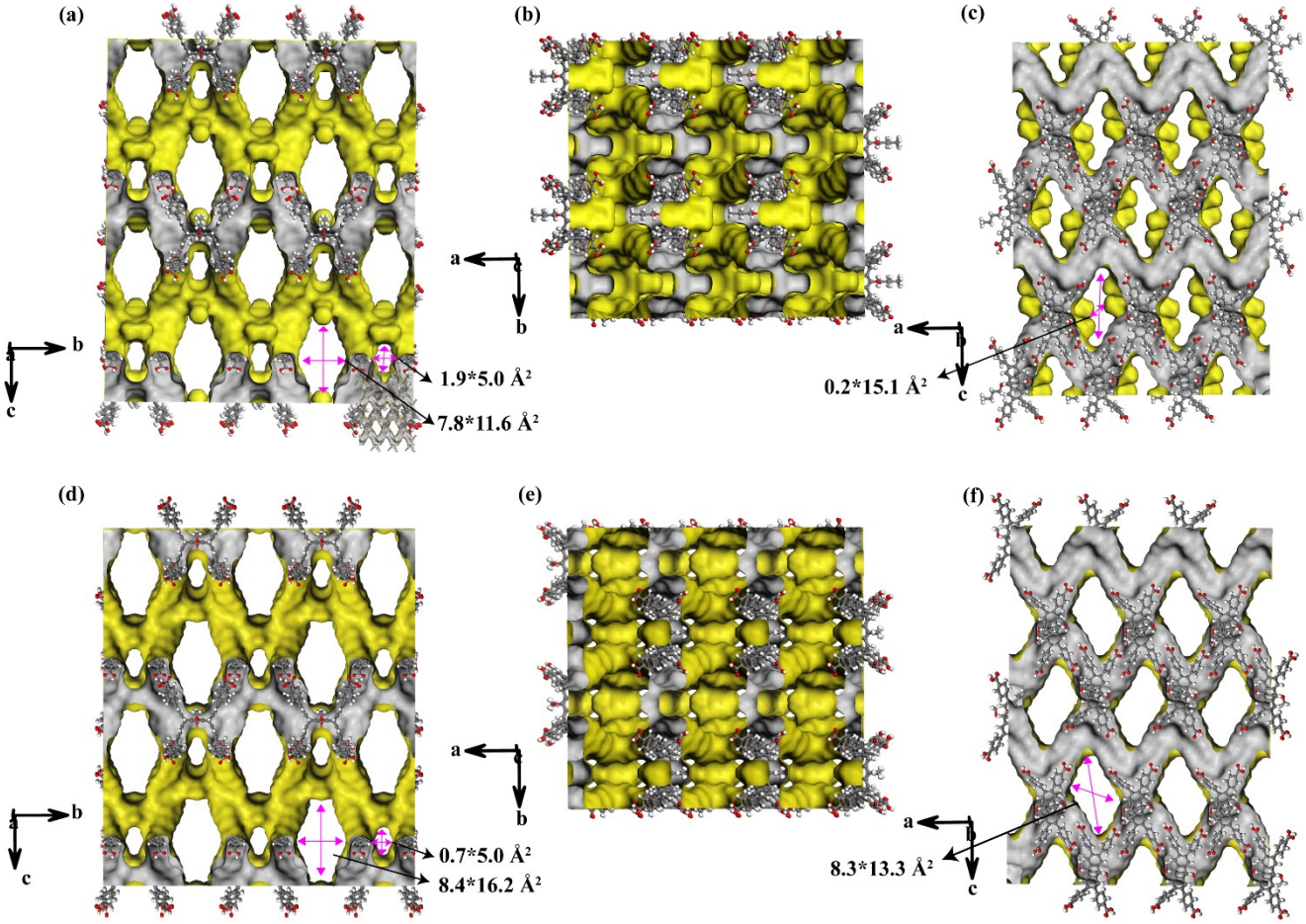

Fig. S5 Visualized surface of the activated void in NKM-HOF-1 showing the pore surfaces of 2D channels heighted as yellow/grey (inner/outer) curved planes (a) along the *a*-axis, (b) along the *c*-axis, (c) along the *b*-axis. Visualized surface of the activated void in NKM-HOF-2 heighted as yellow/grey (inner/outer) curved planes (d) along the *a*-axis, (e) along the *c*-axis, (f) along the *b*-axis.

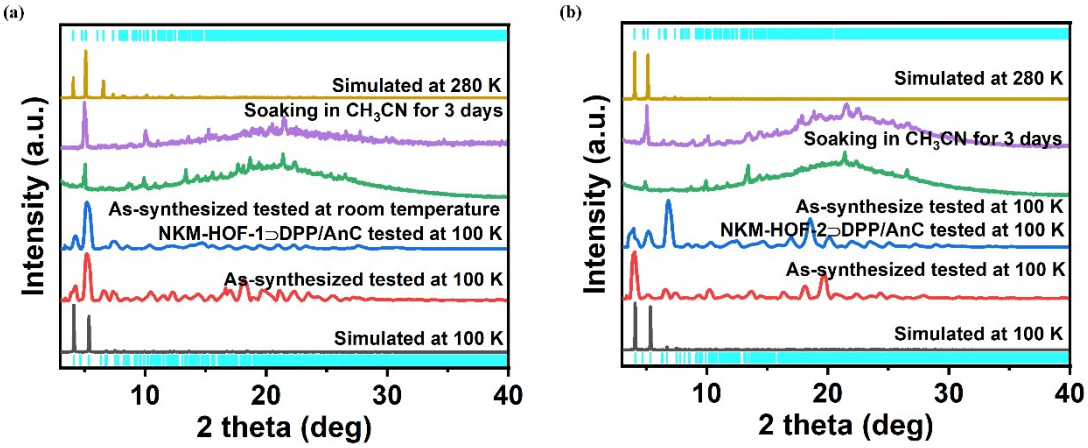

Fig. S6 a) PXRD patterns of NKM-HOF-1 (in ascending order): simulated NKM-HOF-1 from 100 K single crystal data, as-synthesized NKM-HOF-1 measured by a single crystal diffractometer at 100 K, NKM-HOF-1⊃dyes measured by a single crystal diffractometer at 100 K, as-synthesized NKM-HOF-1 measured by a powder X-ray diffractometer at room temperature, NKM-HOF-1 soaked in acetonitrile (CH_3CN) for 3 days, and simulated NKM-HOF-1 from 280 K single crystal data. b) PXRD patterns of NKM-HOF-2 (in ascending order): simulated NKM-HOF-2 from 100 K single crystal data, as-synthesized NKM-HOF-2 measured by a single crystal diffractometer at 100 K, NKM-HOF-2⊃dyes measured by a single crystal diffractometer at 100 K, as-synthesized NKM-HOF-2 measured by a powder X-ray diffractometer at room temperature, NKM-HOF-2 soaked in CH_3CN for 3 days, and simulated NKM-HOF-2 from 280 K single crystal data.

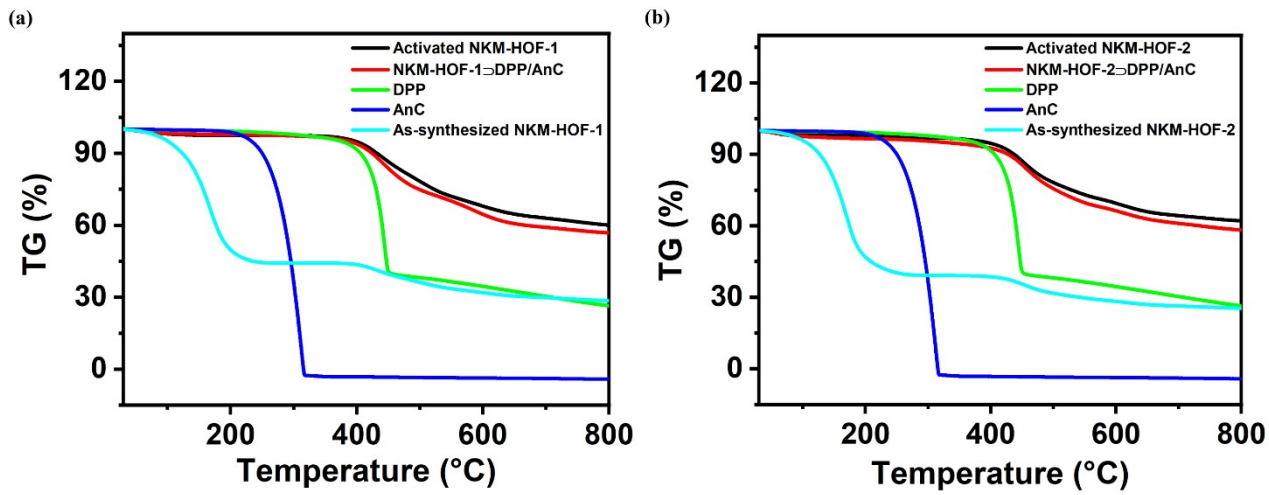

Fig. S7 TG curves of (a) activated NKM-HOF-1, NKM-HOF-1⊃dye, DPP, AnC, and as-synthesized NKM-HOF-1, (b) activated NKM-HOF-2, NKM-HOF-2⊃dye, DPP, AnC, and as-synthesized NKM-HOF-2.

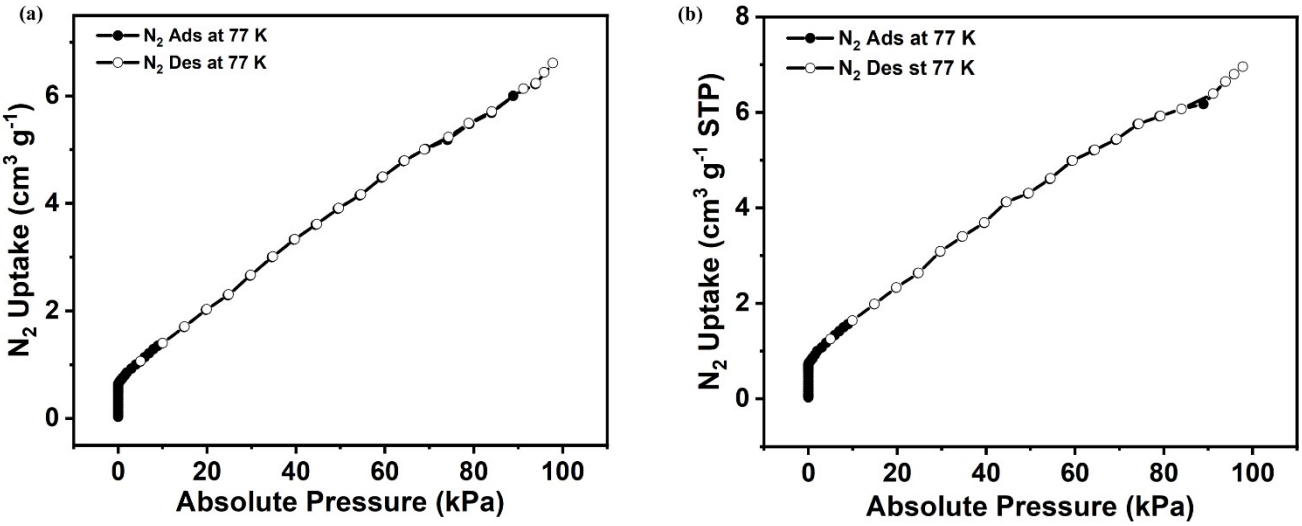

Fig. S8 The N_2 adsorption and desorption isotherms for supercritical CO_2 activated (a) NKM-NOF-1 and (b) NKM-HOF-2 at 77 K.

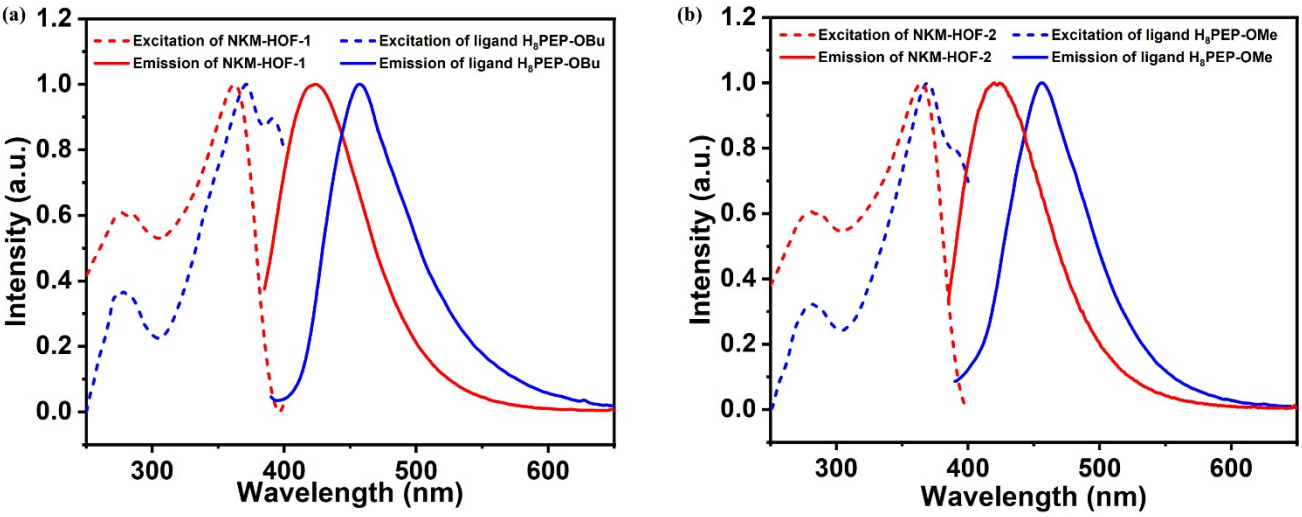

Fig. S9 (a) PL spectra of NKM-HOF-1 and ligand H_8PEP-OBu. (b) PL spectra of NKM-HOF-2 and ligand H_8PEP-OMe.

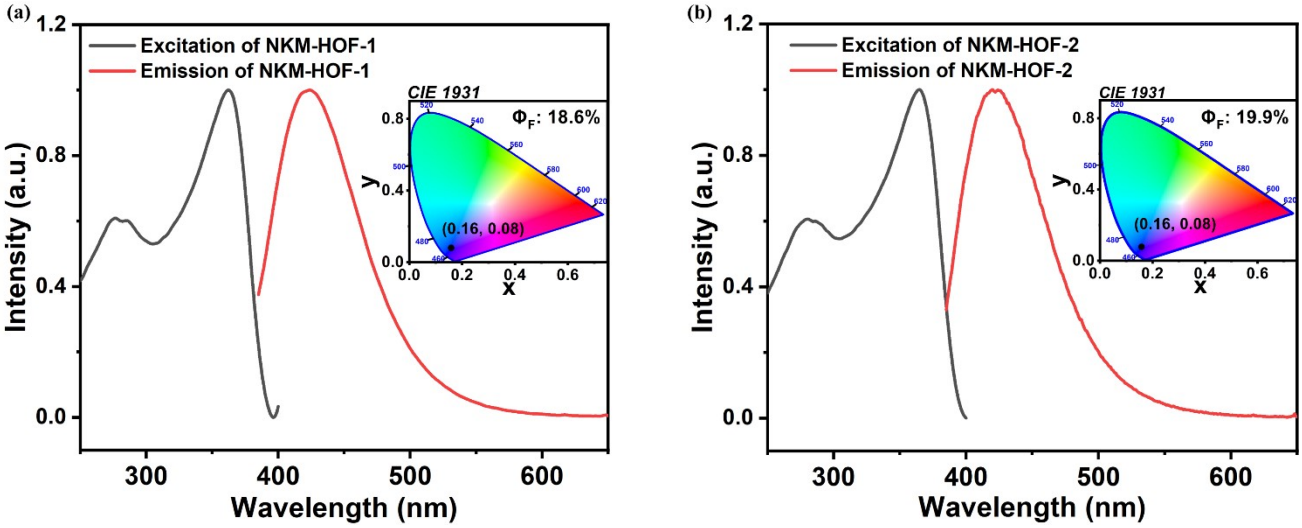

Fig. S10 (a) PL spectra of NKM-HOF-1 (inset: CIE 1931 coordinate of emission of NKM-HOF-1 and quantum yields of NKM-HOF-1). (b) PL spectra of NKM-HOF-2 (inset: CIE 1931 coordinate of emission of NKM-HOF-2 and quantum yields of NKM-HOF-2).

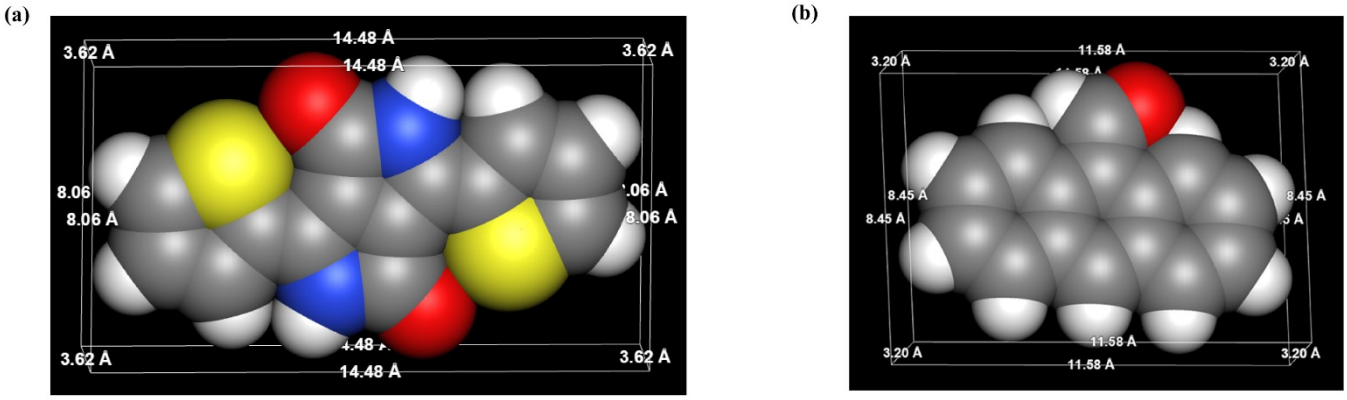

Fig. S11 The molecular size of (a) DPP and (b) AnC.

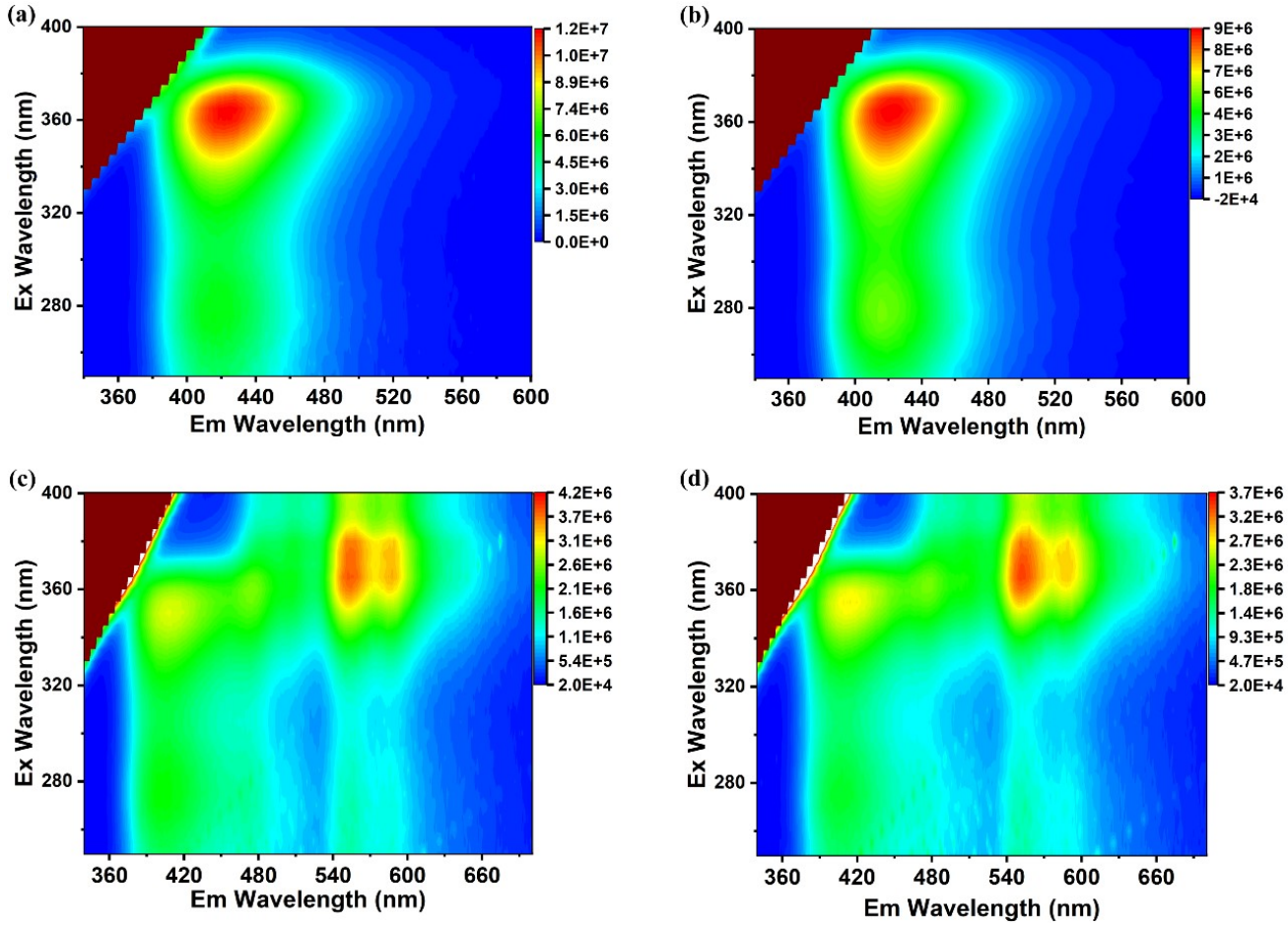

Fig. S12 (a) 3D fluorescence spectra of NKM-HOF-1. (b) 3D fluorescence spectra of NKM-HOF-2. (c) 3D fluorescence spectra of NKM-HOF-1⊃DPP-0.13/AnC-3.5. (d) 3D fluorescence spectra of NKM-HOF-2⊃DPP-0.12/AnC-3.

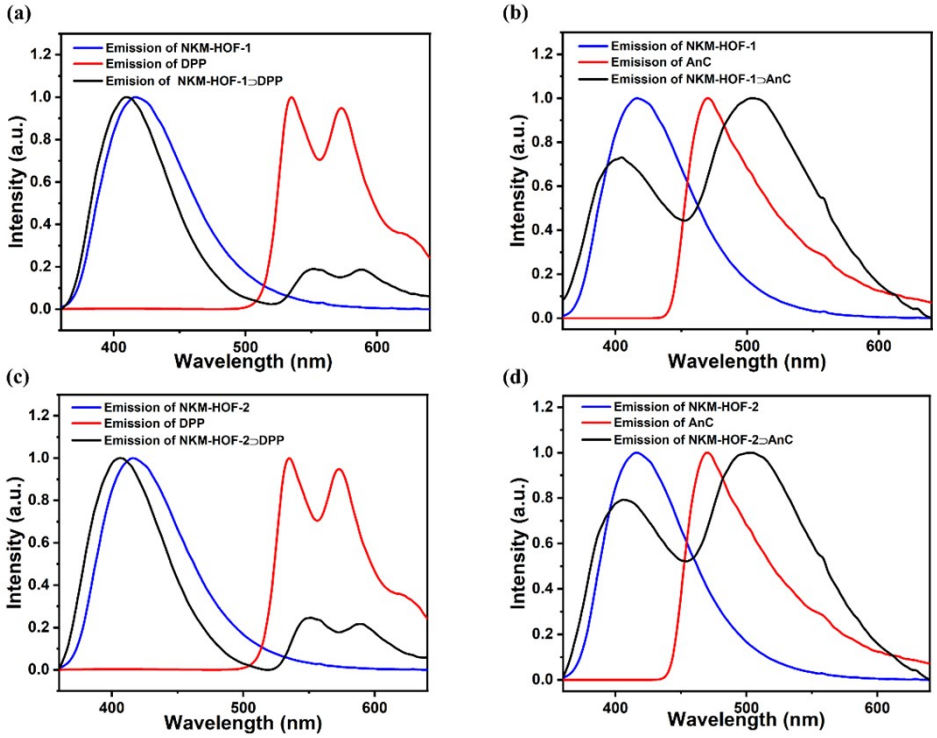

Fig. S13 Under 330 nm excitation, the PL spectra of (a) NKM-HOF-1, the acetonitrile solution of DPP (0.12mmol/L), and NKM-HOF-1⊃DPP; (b) NKM-HOF-1, the acetonitrile solution of AnC (3.8 mmol/L), and NKM-HOF-1⊃AnC; (c) NKM-HOF-2, the acetonitrile solution of DPP (0.12 mmol/L), and NKM-HOF-2⊃DPP; (d) NKM-HOF-2, the acetonitrile solution of AnC (3.8 mmol/L), and NKM-HOF-2⊃AnC.

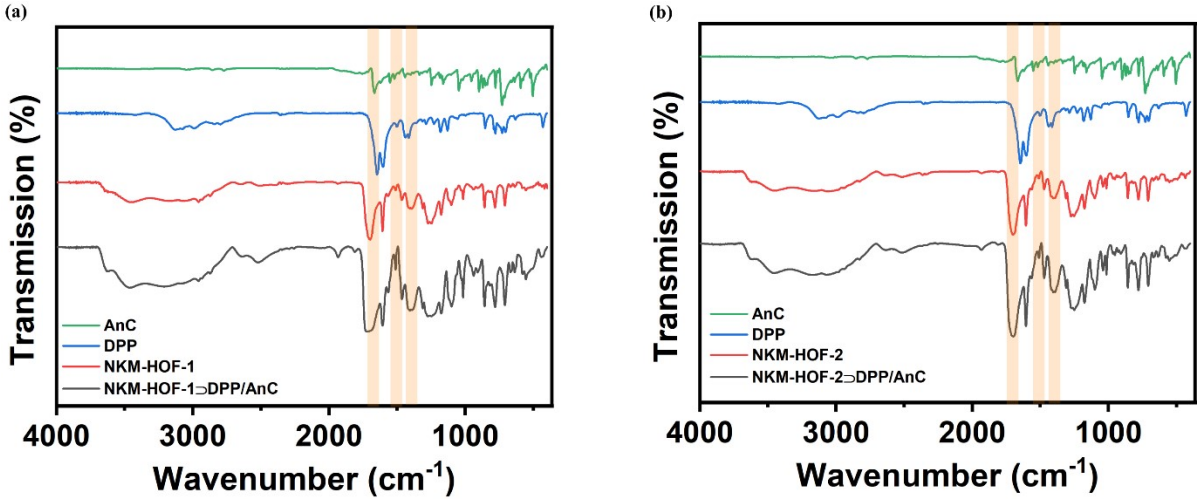

Fig. S14 a) FTIR spectra of AnC, DPP, NKM-HOF-1, and NKM-HOF-1⊃DPP/AnC. b) FTIR spectra of AnC, DPP, NKM-HOF-2, and NKM-HOF-2⊃DPP/AnC.

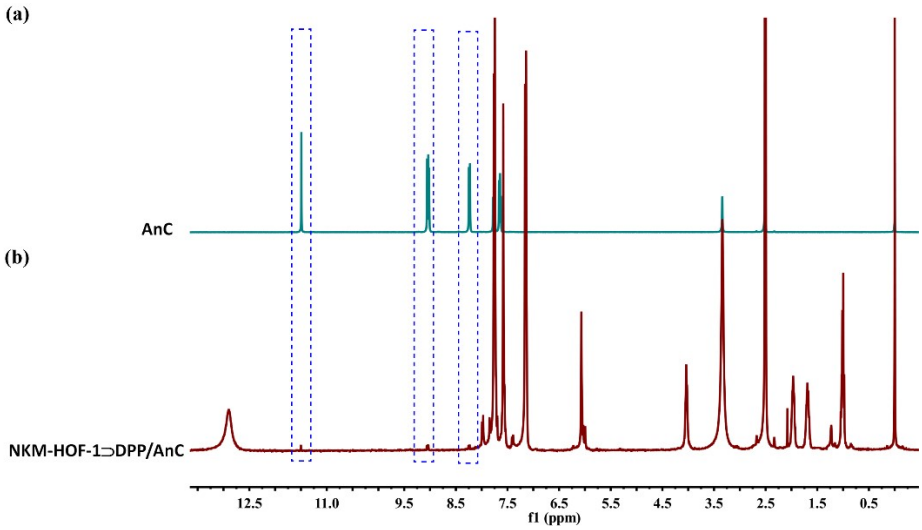

Fig. S15 ^{1}H-NMR spectra of a) AnC and b) NKM-HOF-1⊃DPP/AnC.

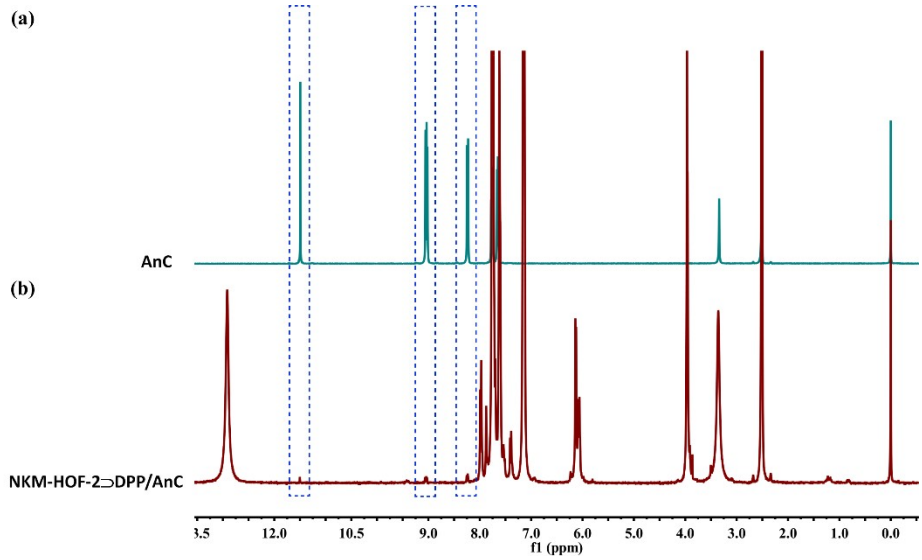

Fig. S16 ^{1}H-NMR spectra of a) AnC and b) NKM-HOF-2⊃DPP/AnC.

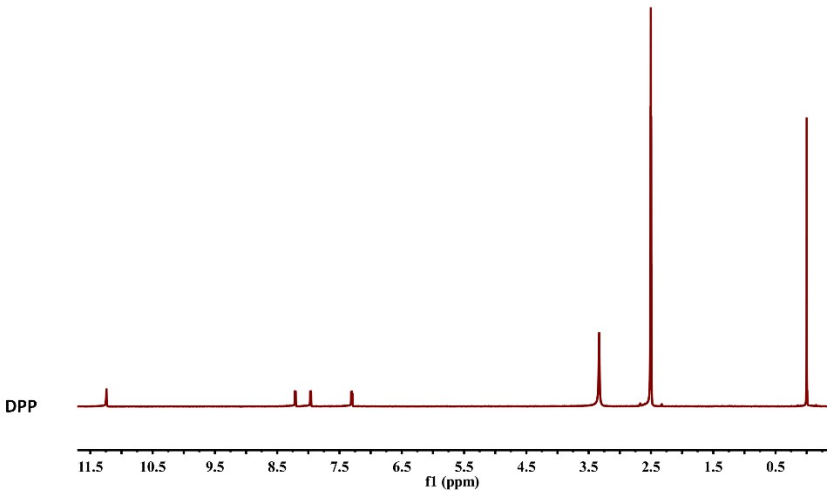

Fig. S17 ^{1}H-NMR spectra of DPP.

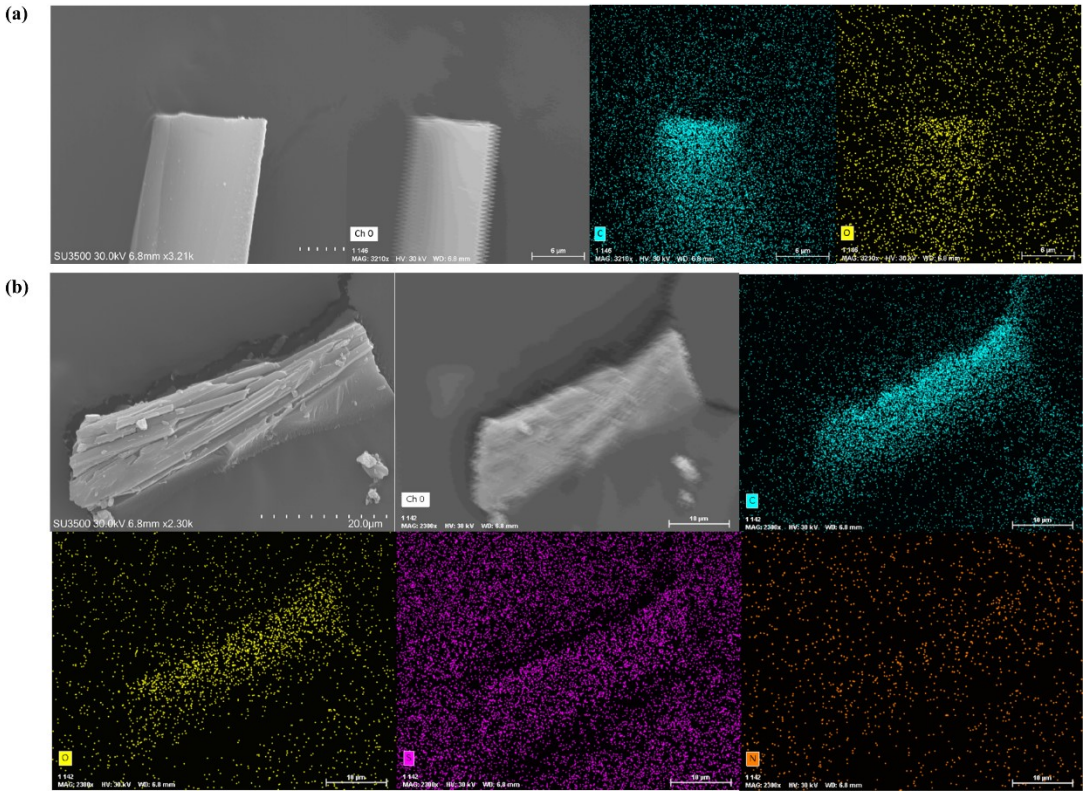

Fig. S18 EDS-mapping images of a) NKM-HOF-1 and b) NKM-HOF-1⊃DPP/AnC.

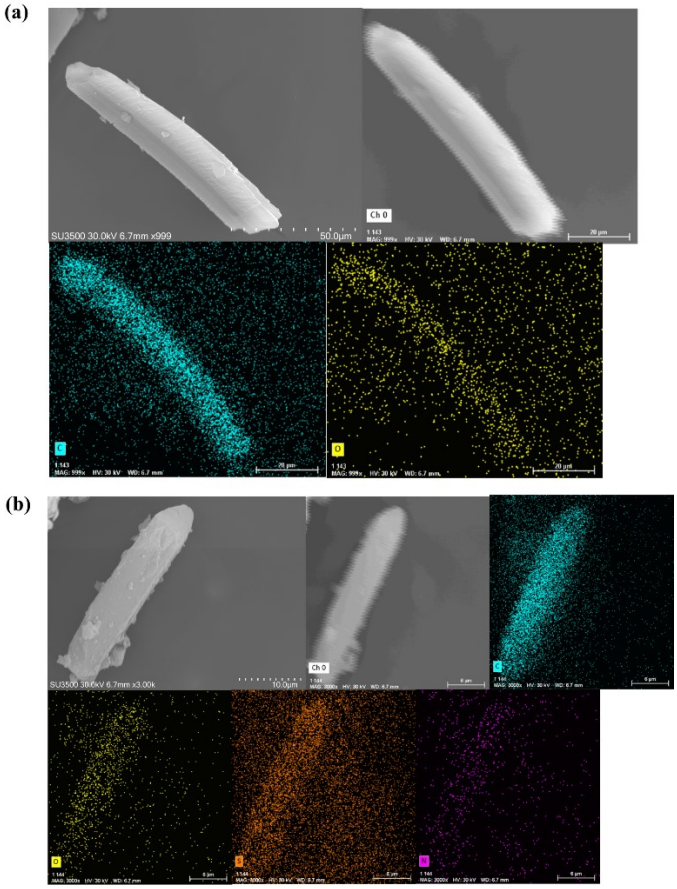

Fig. S19 EDS-mapping images of a) NKM-HOF-2 and b) NKM-HOF-2⊃DPP/AnC.

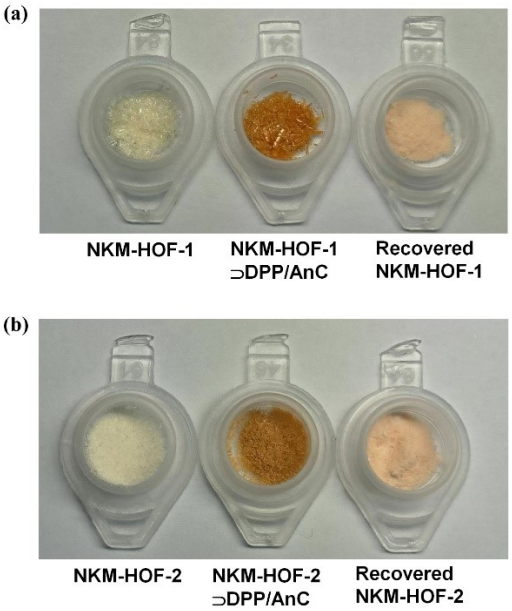

Fig. S20 a) Photographs for samples of NKM-HOF-1, NKM-HOF-1⊃DPP/AnC, and recovered NKM-HOF-1. b) Photographs for samples of NKM-HOF-2, NKM-HOF-2⊃DPP/AnC, and recovered NKM-HOF-2. (NKM-HOFs⊃DPP/AnC exchanged with acetonitrile at 60 °C for 4 days, and the fresh acetonitrile solution was changed three times a day to obtain the recovered sample).

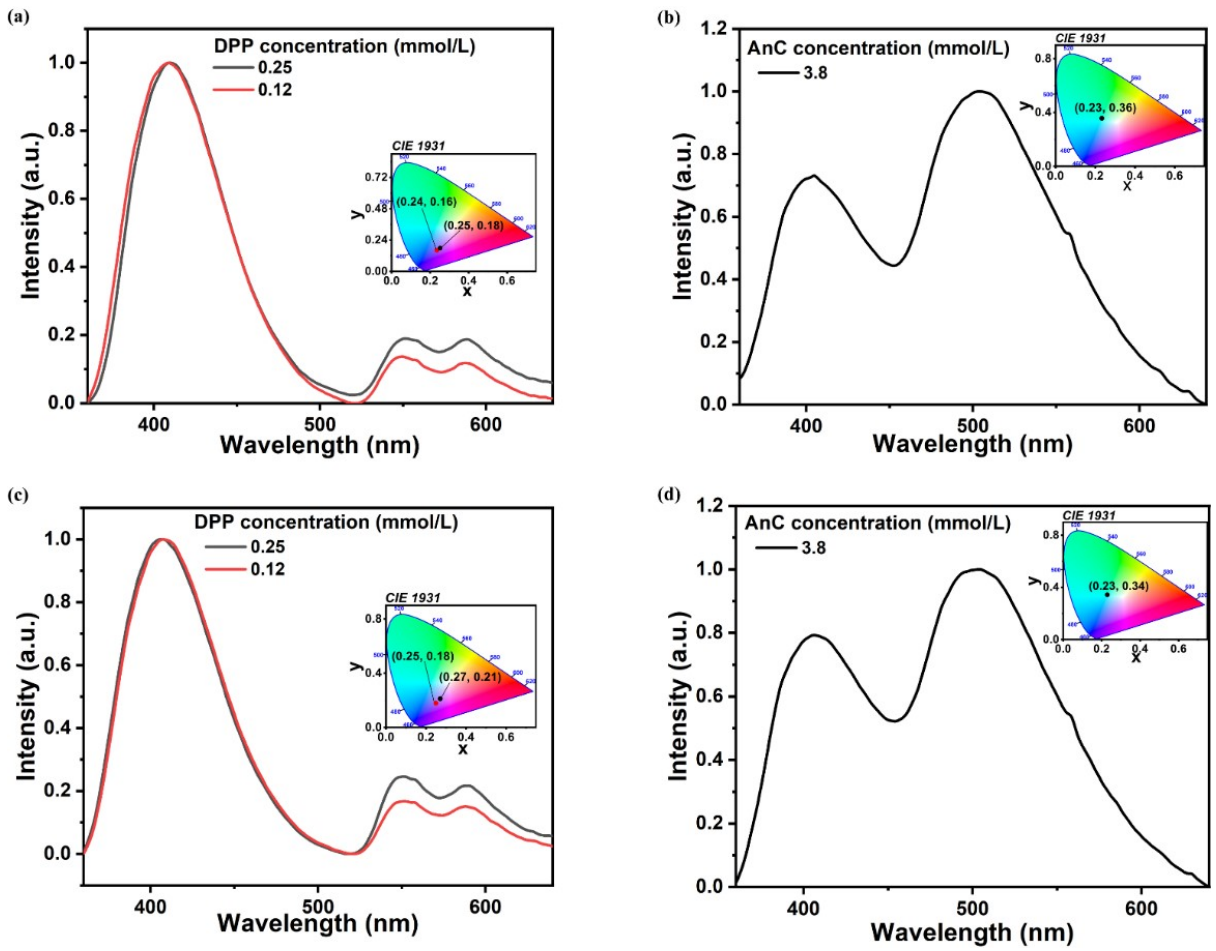

Fig. S21 (a) PL spectra of NKM-HOF-1⊃DPP (inset: CIE 1931 coordinate of emission of NKM-HOF-1⊃DPP). (b) PL spectra of NKM-HOF-1⊃AnC (inset: CIE 1931 coordinate of emission of NKM-HOF-1⊃AnC). (c) PL spectra of NKM-HOF-2⊃DPP (inset: CIE 1931 coordinate of emission of NKM-HOF-2⊃DPP). (d) PL spectra of NKM-HOF-2⊃AnC (inset: CIE 1931 coordinate of emission of NKM-HOF-2⊃AnC).

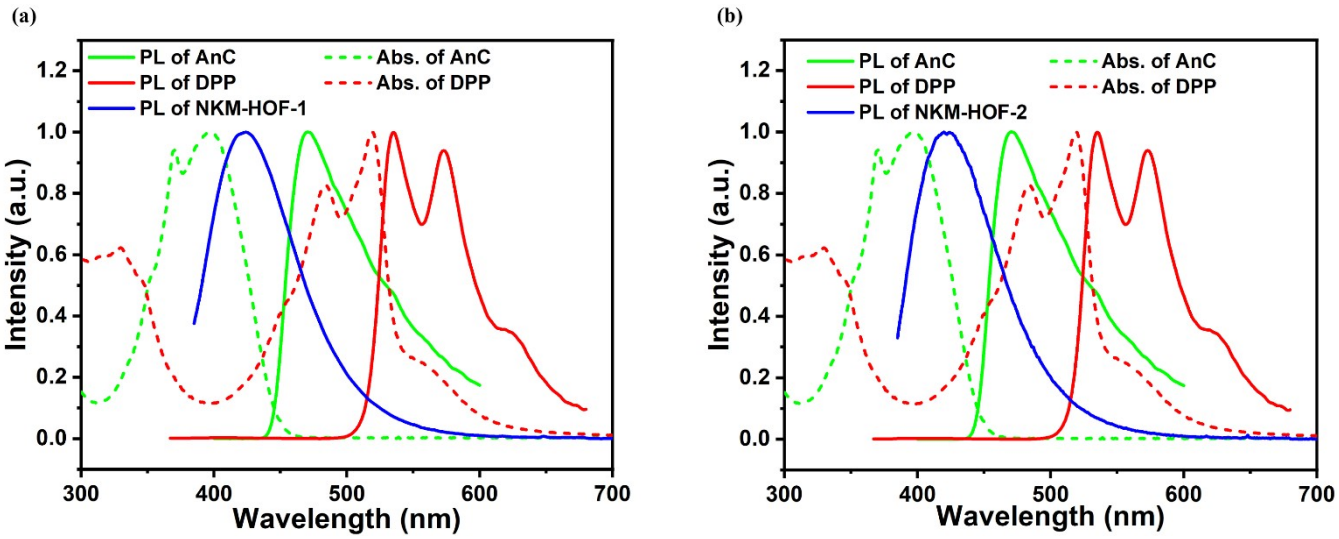

Fig. S22 (a) Absorption and PL spectra of AnC and DPP in acetonitrile solution and PL spectra of NKM-HOF-1 crystal under 330 nm laser excitation. (b) Absorption and PL spectra of AnC and DPP in acetonitrile solution and PL spectra of NKM-HOF-2 crystal under 330 nm laser excitation.

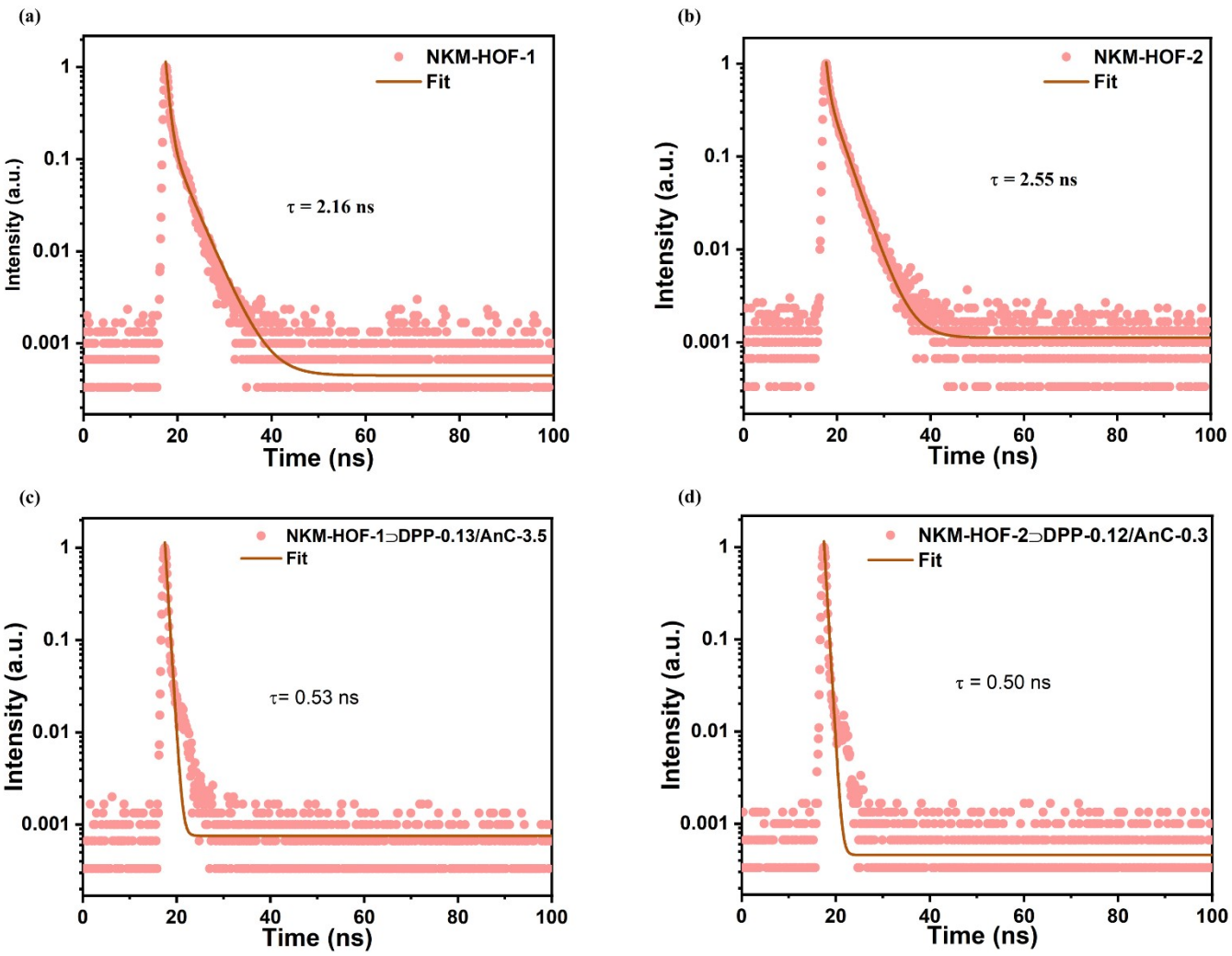

Fig. S23 The decay spectra of 404 nm emission in NKM-HOF-1 (a), NKU-HOF-1⊃DPP-0.13/AnC-3.5 (b), NKM-HOF-2 (c), and NKM-HOF-2⊃DPP-0.12/AnC-3 (d) excited by 375 nm laser.

Table S3 CIE coordinates of NKM-HOF-1⊃DPP/AnC.

sample	CIE coordinates
NKM-HOF-1⊃DPP-0.13/AnC-0.5	(0.2442, 0.1957)
NKM-HOF-1⊃DPP-0.13/AnC-1	(0.2488, 0.2214)
NKM-HOF-1⊃DPP-0.13/AnC-2	(0.2615, 0.2569)
NKM-HOF-1⊃DPP-0.13/AnC-3	(0.2696, 0.2948)
NKM-HOF-1⊃DPP-0.13/AnC-3.5	(0.2853, 0.3287)
NKM-HOF-1⊃DPP-0.13/AnC-4	(0.2938, 0.3639)

Energy transfer efficiency study by decay lifetime

The decreased lifetime of NKM-HOF-1 and NKM-HOF-2 reveals the efficient energy transfer process. The energy transfer efficiency[4] (η_{ET}) and the rate constant of energy transfer (k_{ET}) were calculated through Equation 1 and 2, respectively. τ_{DA} and τ_D are the fluorescence lifetimes of HOF⊃dye and pure HOF materials.

$\eta_{ET} = 1 - (\tau_{DA}/\tau_D)$ (1);

$k_{ET} = \tau_{DA}^{-1} - \tau_D^{-1}$ (2).

Table S4 Fluorescence lifetimes (τ), the rate constant of energy transfer k_{ET}, and Energy transfer efficiency (η_{ET}) and in NKM-HOF-1⊃DPP-0.13/AnC-3.5 and NKM-HOF-2⊃DPP-0.12/AnC-3.

sample	NKM-HOF-1⊃DPP-0.13/AnC-3.5	NKM-HOF-2⊃DPP-0.12/AnC-3
τ_{DA} (ns)	0.53	0.50
τ_D (ns)	2.16	2.55
k_{ET} ($10^{\wedge 9}$ S^{-1})	1.42	1.61
η_{ET}	0.75	0.80

Table S5 Fluorescence lifetimes (τ) and quantum yields of NKM-HOF-1, NKM-HOF-2, NKM-HOF-1⊃DPP-0.13/AnC-3.5, and NKM-HOF-1⊃DPP-0.12/AnC-3.

sample	NKM-HOF-1	NKM-HOF-2	NKM-HOF-1⊃DPP-0.13/AnC-3.5	NKM-HOF-2⊃DPP-0.12/AnC-3
T (ns)	2.16	2.55	0.53	0.50
Quantity yield	18.64%	19.94%	7.08%	8.71%

Table S6 CIE coordinates of NKM-HOF-2⊃DPP/AnC.

sample	CIE coordinates
NKM-HOF-1⊃DPP-0.12/AnC-0.5	(0.2581, 0.2085)
NKM-HOF-1⊃DPP-0.12/AnC-2	(0.2957, 0.2919)
NKM-HOF-1⊃DPP-0.12/AnC-2.5	(0.3013, 0.3145)
NKM-HOF-1⊃DPP-0.12/AnC-3	(0.3162, 0.3374)
NKM-HOF-1⊃DPP-0.12/AnC-3.5	(0.3209, 0.3498)
NKM-HOF-1⊃DPP-0.12/AnC-4	(0.3235, 0.3625)

References

[1] CryaAlisPro, Aligent Technologies. Version 1.171.36.31

[2] G. M. Sheldrick, *Acta. Crystallogr. Sect. A*. **2015**, *71*, 3-8.

[3] O. V . Dolomanov, L. J. Bourhis, R. J. Gildea, J. A. K. Howard, H. Puschmann, *J. Appl. Cryst*. **2009**, *42*, 339-341.

[4] M. Huang, Z. Liang, J. Huang, Y. Wen, Q.-L. Zhu, X. Wu, *ACS Appl. Mater. Interfaces* **2023**, *15*, 11131-11140.